Merging Neutron Star – Black Hole Binaries

M. Ruffert* and H.-Th. Janka†

*University of Edinburgh, Edinburgh EH93JZ, Scotland, U.K.
†MPI für Astrophysik, Postfach 1317, 85741 Garching, Germany

Abstract. We report on ongoing investigations of the merger model for the central engine of gamma-ray bursts and show first results of a new set of simulations for neutron star black hole binaries. The masses of the neutron star and black hole are the same in all cases, but we change the numerical resolution and the gravitational potential of the black hole by using descriptions that follow Paczyński & Wiita (1980) and Artemova et al. (1996). Since our code is basically Newtonian, this procedure is supposed to mimic the general relativistic effects that are associated with the existence of an innermost stable orbit and the variation of this orbit and of the horizon radius with the spin and the growing mass of the accreting black hole. The neutron star, which initially is in orbit about the black hole, is tidally disrupted but in several cases the remnant manages to temporarily move to a more eccentric orbit. A second and final episode of mass transfer follows, producing the standard outcome of a high-density torus around the black hole. Our simulations still need to be analysed with respect to the neutrino-antineutrino annihilation luminosities, but we expect similar values as in the double neutron star models.

INTRODUCTION

Although most recent observations and measurements of gamma-ray bursts favour the collapsar model as central engine, these detections are all instances of the "long" type of gamma-ray burst (GRB). Much less is known about the "short" GRBs, except that their duration and hardness are distinct from those of long GRBs (cf. Briggs, 2002). While the collapsar model works well for the long GRBs it does have difficulty in generating short burst durations (cf. Woosley, 2002). The model involving the merger of compact objects, i.e. neutron stars and black holes, not only roughly matches the observed occurrence rates, but the natural (dynamic) timescales (ms) are of the order of the variability timescale of short GRBs.

We are now extending our previous investigations to look at the merging of a binary consisting of a neutron star and a black hole (NS-BH). In previous work of merging double neutron star binaries (NS-NS) we showed that neutrino-antineutrino annihilation could provide the luminosity necessary to power a short GRB, if that neutrino luminosity is sustained for the typical durations of short GRBs, i.e. 0.1–1 sec. An asymmetric merger involving a black hole and a neutron star promises a priori to yield a more massive torus around the black hole, since the black hole is already present and no mass needs to be 'lost' to first form the black hole. On the other hand, the deeper potential well present from the outset might facilitate more mass to be accreted anyway. Numerous effects of similar nature, e.g. deeper potential well allows more energetic neutrino emission, etc., act to both increase as well as decrease the clean energy finally available for the fireball.

Our main initial aim when performing these computations is to compare the NS-BH results — torus mass, accretion rates, neutrino emission, annihilation luminosities — to the results produced by NS-NS mergers. The NS-BH results will depend on additional parameters specific to these models, e.g. mass and spin of black hole, and these will have to be varied, too, to assess their influence.

The conference talk and consequently this proceedings contribution can only report on preliminary results, since the calculations are still in progress. Thus results are not available yet for all models of interest and only a few models are completed.

NUMERICAL PROCEDURES AND INITIAL CONDITIONS

Numerical Procedures

Here we will only summarise the computational procedures that we used. Details of the hydrodynamic method as well as the neutrino relevant algorithms can be found in Ruffert et al. (1996, 1997). The nested grid was described by Ruffert & Janka (1998) and Ruffert (1992). The implementation of the black hole was explained in Ruffert & Janka (1999), Eberl (1998) and Janka et al. (1999).

The hydrodynamical simulations were done with a code based on the Piecewise Parabolic Method (PPM) developed by Colella & Woodward (1984). The code is basically Newtonian, but contains the terms necessary to describe gravitational-wave emission and the corresponding back-reaction on the hydrodynamical flow (Blanchet et al 1990). The gravitational potential and other quantities that follow from a Poisson equation are obtained from fast Fourier transforms. Other spatial derivatives are evaluated as standard centred differences on the grid.

In order to describe the thermodynamics of the neutron star matter, we use the EoS of Lattimer & Swesty (1991) for a compressibility modulus of bulk nuclear matter of $K = 180\,\mathrm{MeV}$ in tabular form. Use of a physical EoS instead of a simple ideal gas law implies that the adiabatic index is a function of space, i.e. of density, temperature and composition in the star, as well as of time, i.e. the value of the adiabatic index of the bulk of the matter changes when the neutron star strips some of its mass.

Energy loss and changes of the electron abundance due to the emission of neutrinos and antineutrinos are taken into account by an elaborate “neutrino leakage scheme”. The energy source terms contain the production of all types of neutrino pairs by thermal processes and additionally of electron neutrinos and antineutrinos by lepton captures onto baryons. The latter reactions act as sources or sinks of lepton number, too, and are included as source terms in a continuity equation for the electron lepton number. Matter is rendered optically thick to neutrinos due to the main opacity producing reactions, which are neutrino-nucleon scattering and absorption of electron-type neutrinos onto nucleons.

The presented simulations were done on multiply nested and refined grids. With an only modest increase in CPU time, the nested grids allow one to simulate a substantially larger computational volume while at the same time they permit a higher local spatial resolution of the merging stars. The former is important to follow the fate of matter that is flung out to distances far away from the merger site either to become unbound or to eventually fall back. The latter is necessary to adequately resolve the strong shock fronts and steep discontinuities of the plasma flow that develop during the collision. The procedures used here are based on the algorithms that can be found in Berger & Colella (1989), Berger (1987) and Berger & Oliger (1984). Each grid had 64^3 or 128^3 zones, the size of the smallest zone was $\Delta x = \Delta y = \Delta z =$ 1.27 or 0.64 km, respectively. The zone sizes of the next coarser grid levels were doubled to cover a volume of 648 km side length. We used 4 nested grids.

TABLE 1. Models that have been or will be computed, with their characterising parameters. N is the number of grid zones per dimension in the orbital plane, L the size of the largest grid, a_0 the initial centre to centre distance of the neutron star from the black hole. “BH spin” indicates the magnitude of the Kerr parameter used in the phenomenological model by Artemova et al. (1996) to mimic rotating black holes.

Model	N	Potential	L km	BH spin	a_0 km
Newt	64	Newton	648	0	50.
Newt2	128	Newton	648	0	50.
PaWi	64	PaWi	648	0	58.
PaWi2	128	PaWi	648	0	58.
Ker6	64	Kerr	648	+0.6	55.
Ker6/2	128	Kerr	648	+0.6	55.
Ker9	64	Kerr	648	+0.9	54.
Ker9/2	128	Kerr	648	+0.9	54.
Ret9	64	Kerr	648	-0.9	63.
Ret9/2	128	Kerr	648	-0.9	63.

The black hole was modeled as a vacuum sphere on the grids. Any gaseous matter that flowed into that region was taken out of the grids and the mass, velocity and angular momentum of the black hole changed by the appropriate amounts. The potential of the black hole was approximated either by a purely Newtonian dependence (i.e. $1/r$), or a Paczyński-Wiita type potential (i.e. $1/(r - r_\mathrm{s})$, cf. Paczyński & Wiita, 1980) which models the effect of the last stable orbit, or by its extension by Artemova et al. (1996) which mimics the effect of a rotating (Kerr) black hole on the location of the innermost stable circular orbit. For rotating black holes, the radii of both the event horizon (r_h) as well as of the last stable circular orbit (r_o) depend on the angular momentum via the Kerr parameter. The pseudo-potential diverges at the horizon. Therefore the radius of the vacuum sphere was chosen to be the arithmetic average $(r_\mathrm{h} + r_\mathrm{o})/2$.

With these new models we have not yet performed the post-processing step, to evaluate the neutrino-antineutrino ($\nu\bar{\nu}$) annihilation in the surroundings of the merged stars. This can only be performed after the hydrodynamical evolution is complete and will allow us to construct maps showing the local energy deposition rates per unit volume when a quasi-steady state has been reached. Spatial integration finally yields the total rate of energy deposition outside the neutrino emitting high-density regions.

Initial conditions

We considered neutron stars with a baryonic mass of about 1.63 $M_\odot$ and the black hole mass was initially

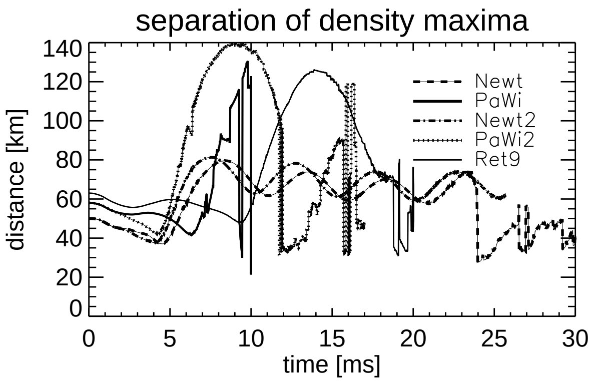

FIGURE 1. Distance of centre of neutron star from centre of black hole as function of time for several models.

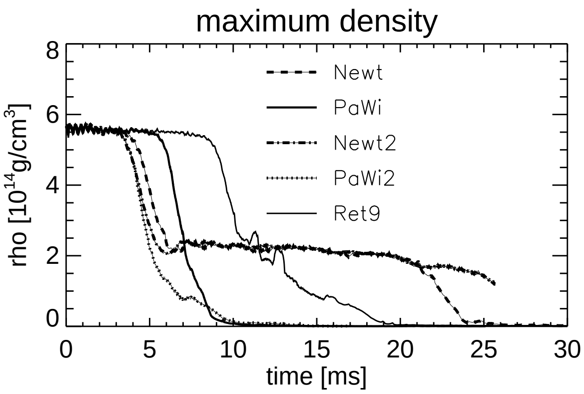

FIGURE 2. Value of maximum density within the computational volume as function of time for several models.

chosen to be 2.5 $M_\odot$. The black hole mass obviously increases during the simulation as it absorbs matter from the neutron star. With the equation-of-state that we used the neutron star has a radius of approximately 15 km.

The distributions of density ρ and electron fraction $Y_e \equiv n_e/n_b$ (with n_e being the number density of electrons minus that of positrons, and n_b the baryon number density) were taken from a one-dimensional model of a cold, deleptonized (neutrino-less) neutron star in hydrostatic equilibrium and were the same as in Ruffert et al. (1996). The initial central temperature was set to a value of typically a few MeV, the temperature profile decreasing towards the surface such that the thermal energy was much smaller than the degeneracy energy of the matter.

We prescribed the initial orbital velocities of the coalescing neutron star and black hole according to the motions of point masses, as computed from the quadrupole formula. The tangential components of the velocities of the centres of the compact objects correspond to Kepler velocities on circular orbits, while the radial velocity components reflect the emission of gravitational waves leading to the inspiral of the orbiting bodies. No additional spin was added, so the neutron star can be considered as "irrotational".

Table 1 gives a list of ongoing merger simulations. "PaWi" refers to a Paczyński-Wiita type potential (Paczyński & Wiita, 1980) while "Kerr" indicates the use of the Artemova type potential (Artemova et al., 1996). The Table also lists the initial centre-to-centre distance between black hole and neutron star. Since we do not relax the neutron stars at the start the simulations the initial distances have to be chosen sufficiently large that most of the induced oscillations have been damped away by numerical viscosity before the dynamical phase of the merging is reached.

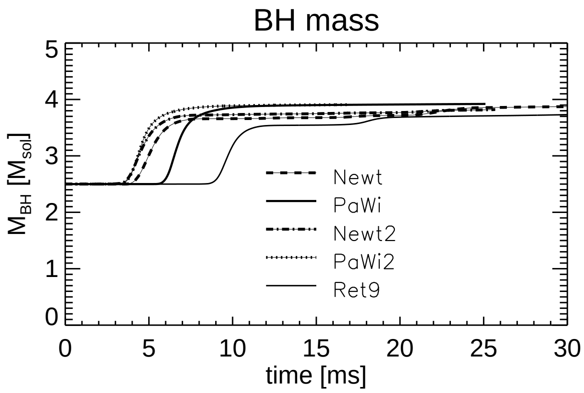

FIGURE 3. Black hole mass as function of time for several models.

RESULTS

Figs. 1 and 2 show distinct episodic phases of the merging process. First, the orbits shrink slowly while the neutron star retains its mass and density structure (constant maximum density except for small-amplitude oscillations). A rapid mass transfer from the neutron star to the black hole follows and is shut off again within 1–2 ms (compare also Figs. 3, 4 and 5); accretion rates of nearly 10^3 $M_\odot$/s are reached during this time. The neutron star is then flung into an eccentric orbit which will at first take it away from the black hole but eventually they meet again (similar behaviour has been reported by Lee, 2000). Note that the neutron star in models Newt and Newt2 orbits several times before the second and final plunge into the black hole, and during that time its maximum density is around $2 \cdot 10^{14}$ g/cm^3, and its mass is about 0.25 $M_\odot$. Note also the rough similarities between the results of the low-resolution model Newt and the high-resolution model Newt2. On the contrary, models PaWi and PaWi2 do not seem to agree that well, indi-

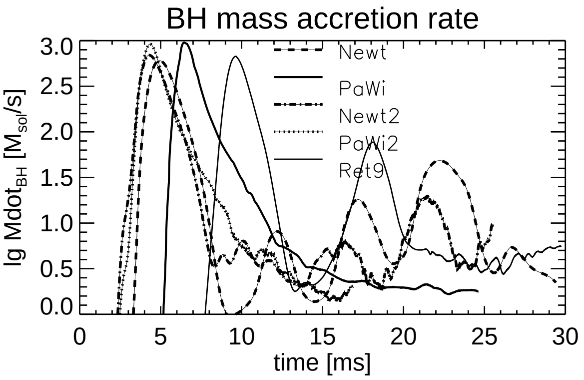

FIGURE 4. Black hole mass accretion rate as function of time for several models.

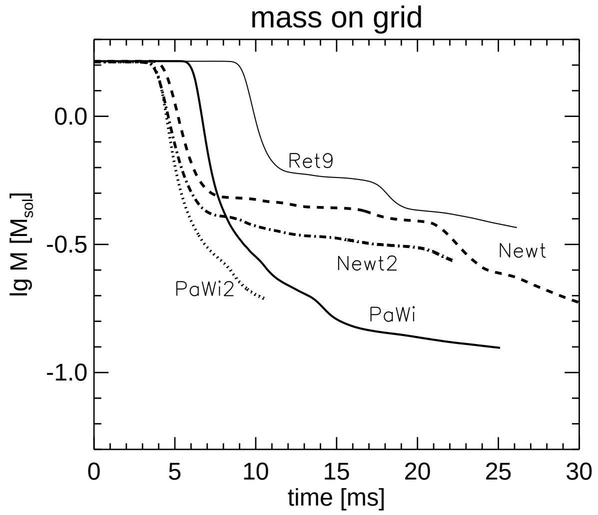

FIGURE 5. Mass of gas within the computational volume as function of time for several models.

cating the need for even higher numerical resolution.

Although most of the gaseous matter is accreted by the black hole, some becomes unbound and escapes. Fig. 6 displays logarithmically the amount of unbound mass as function of time, typically several percent of a solar mass by the end of the simulation. Together with mass the black hole accretes angular momentum, too. This is reflected in the time dependence of the rotational (Kerr) parameter shown in Fig. 7. In all models except model Ker9 the value of their rotational parameter increases. For these models the accreted matter spins up the black hole in the direction of the rotation of the disk (for the black hole with the retrograde spin in model Ret9 this means a spin-down). Only the black hole in model Ker9 is initially spinning so rapidly, that the accreted matter has less specific angular momentum. Note that this regime is highly relativistic and general relativistic

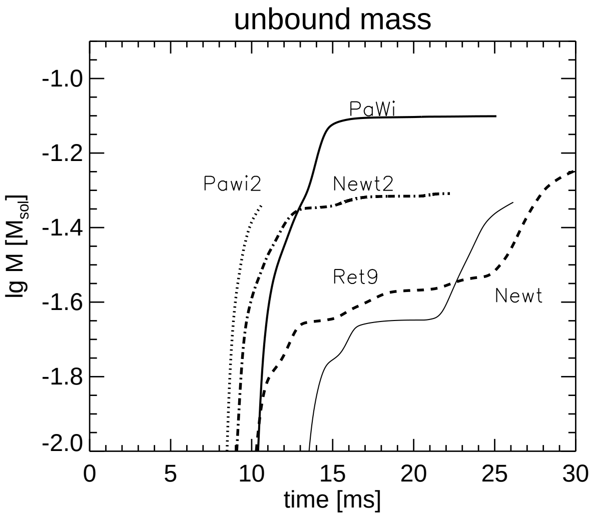

FIGURE 6. Mass of gas that is unbound when it leaves the computational volume for several models.

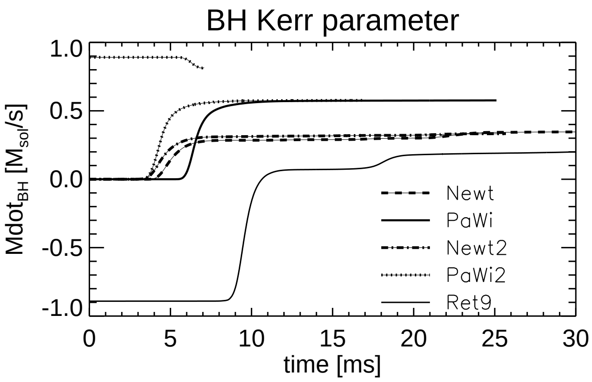

FIGURE 7. Black hole rotational (Kerr) parameter as function of time for several models. The topmost line shows model Ker9.

effects are expected to be strongest here.

The neutrino luminosities (Fig. 8) are roughly similar to what has been reported previously (Ruffert & Janka, 1999; Janka et al. 1999): they rise up to several 10^{53} erg/s. Given a similar geometry (torus around black hole) we anticipate similar neutrino-antineutrino annihilation luminosities and finally available clean energies for the fireball.

The gravitational wave luminosity is shown as function of time plotted logarithmically in Fig. 9 and linearly in Fig. 10. These results are to be accepted with caution, since our code is Newtonian. While the maximum luminosity is fairly similar, around 3–$7 \cdot 10^{55}$ erg/s, the subsequent evolution depends sensitively on whether a remnant neutron star remains in orbit or not. If so, during the period before the remnant gets tidally disrupted, a

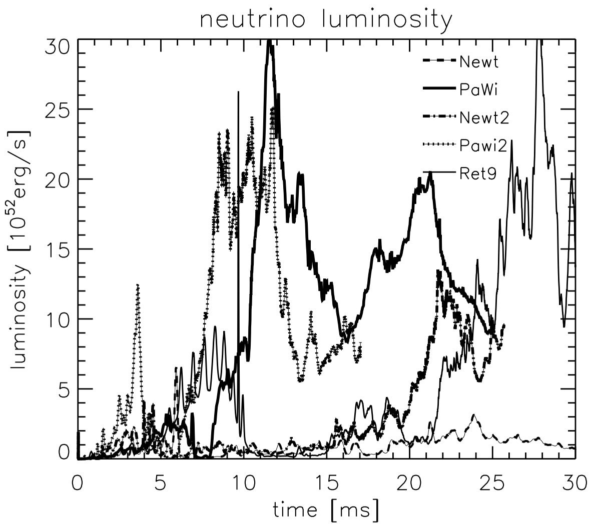

FIGURE 8. Total neutrino luminosity as function of time for several models.

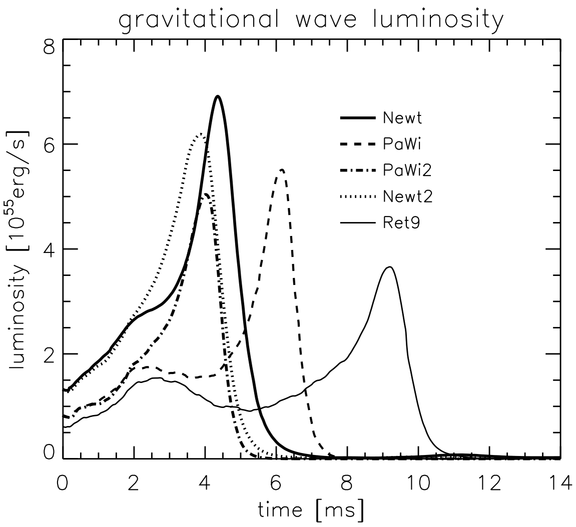

FIGURE 10. Gravitational wave luminosity as function of time for several models.

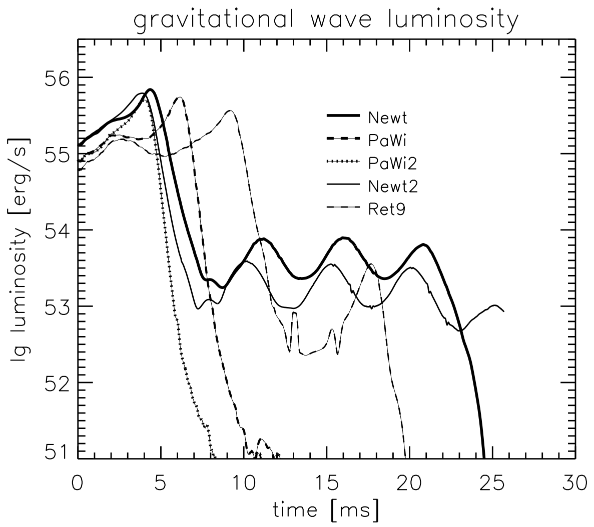

FIGURE 9. Gravitational wave luminosity as function of time for several models.

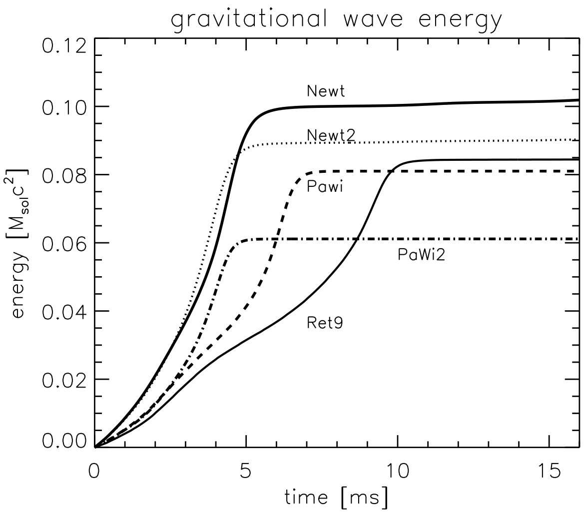

FIGURE 11. Integrated emitted gravitational wave energy as function of time for several models.

residual gravitational wave luminosity is present but at a reduced level of approximately two orders of magnitude below the peak value. The time-integrated energy carried away by gravitational waves is shown in Fig. 11.

CONCLUSIONS

We show the first results of ongoing simulations investigating the mergers of neutron star-black hole binaries with the gravitational potential of the black hole being generalized to account for the effects of the existence of an innermost stable circular orbit. The emission of neutrinos is included to ascertain the viability of this model as a possible central engine of gamma-ray bursts. In some cases a low-mass neutron star remnant seems to be left over after a first episode of mass transfer. This remnant eventually gets tidally disrupted, too. Some of the quantities we display are the maximum density, the mass and mass accretion rate of the black hole, and the neutrino and gravitational wave luminosities.

ACKNOWLEDGMENTS

MR gratefully acknowledges support by a PPARC Advanced Fellowship and HTJ by the Sonderforschungsbereich 375 on "Astroparticle Physics" of the Deutsche Forschungsgemeinschaft. Most of the computations reported here were performed using the UK Astrophysical Fluids Facility (UKAFF).

REFERENCES

1. Artemova I.V., Björnsson G., Novikov I.D., 1996, ApJ 461, 565.
2. Berger M.J. 1987, J. Numer. Anal., 24, 967.
3. Berger M.J., & Colella P. 1989, J. Comput. Phys., 82, 64.
4. Berger M.J., & Oliger J. 1984, J. Comput. Phys., 53, 484.
5. Blanchet L., Damour T., & Schäfer G. 1990, MNRAS, 242, 289.
6. Briggs M.E., 2002, these proceedings.
7. Colella P., & Woodward P.R. 1984, J. Comput. Phys., 54, 174.
8. Janka H.-T., Eberl T., Ruffert M., & Fryer C.L. 1999, ApJ, 527, L39.
9. Eberl T. 1998, Diploma Thesis, Technical University Munich.
10. Lattimer J.M., & Swesty, F.D. 1991, Nucl. Phys., A535, 331
11. Lee W.H. 2000, MNRAS 318, 606.
12. Paczyński B., & Wiita P.J. 1980, A&A, 88, 23.
13. Ruffert M. 1992, A&A, 265, 82.
14. Ruffert M., & Janka H.-T. 1998, A&A, 338, 535.
15. Ruffert M., & Janka H.-T. 1999, A&A, 344, 573.
16. Ruffert M., Janka H.-T., & Schäfer G. 1996, A&A, 311, 532.
17. Ruffert M., Janka H.-T., Takahashi K., & Schäfer G. 1997, A&A, 319, 122.
18. Woosley S., 2002, these proceedings.